Published for SISSA by Springer
Received: January 10, 2014
Revised: May 27, 2014
Accepted: June 12, 2014
Published: July 11, 2014

Impact of a four-zero Yukawa texture on $h \to \gamma\gamma$ and γZ in the framework of the Two Higgs Doublet Model Type III

A. Cordero-Cid,[a] **J. Hernández–Sánchez,**[b] **C.G. Honorato,**[c] **S. Moretti,**[d,e] **M.A. Pérez**[c] **and A. Rosado**[f]

[a] *Fac. de Cs. de la Electrónica, Benemérita Universidad Autónoma de Puebla, Apdo. Postal 542, 72570 Puebla, Puebla, México*
[b] *Fac. de Cs. de la Electrónica, Benemérita Universidad Autónoma de Puebla, Apdo. Postal 542, 72570 Puebla, Puebla, México and Dual C-P Institute of High Energy Physics, México.*
[c] *Departamento de Física, CINVESTAV, Apdo. Postal 14-740, 07000 México, D. F., México.*
[d] *School of Physics and Astronomy, University of Southampton, Highfield, Southampton SO17 1BJ, United Kingdom*
[e] *Particle Physics Department, Rutherford Appleton Laboratory, Chilton, Didcot, Oxon OX11 0QX, United Kingdom*
[f] *Instituto de Física, BUAP, Apdo. Postal J-48, C.P. 72570 Puebla, Pue., México.*

E-mail: acordero@ece.buap.mx, jaime.hernandez@correo.buap.mx, carlos_honorato@ymail.com, s.moretti@soton.ac.uk, mperez@fis.cinvestav.mx, rosado@ifuap.buap.mx

Abstract: We study the substantial enhancement, with respect to the corresponding Standard Model rates, that can be obtained for the branching ratios of the decay channels $h \to \gamma\gamma$ and $h \to \gamma Z$ within the framework of the Two Higgs Doublet Model Type III, assuming a four-zero Yukawa texture and a general Higgs potential. We show that these processes are very sensitive to the flavor pattern entering the Yukawa texture and to the triple coupling structure of the Higgs potential, both of which impact onto the aforementioned decays. We can accommodate the parameters of the model in such a way to obtain the $h \to \gamma\gamma$ rates reported by the Large Hadron Collider and at the same time we get a $h \to \gamma Z$ fraction much larger than in the Standard Model, indeed within experimental reach. We present some scenarios where this phenomenology is realized for spectrum configurations that are consistent with current constraints. We also discuss the possibility of obtaining a light charged Higgs boson compatible with all such measurements, thereby serving the purpose of providing a hallmark signal of the scenario considered.

Keywords: Higgs Physics, Beyond Standard Model

ArXiv ePrint: 1312.5614

doi:10.1007/JHEP07(2014)057

JHEP07(2014)057

Contents

JHEP07(2014)057

1 Introduction

New physics effects in the radiative decays of Higgs bosons have been studied for more than twenty years [1, 2]. In particular, already within the effective Lagrangian approach [3], it was pointed out that anomalous contributions to the Standard Model (SM) vertices $WW\gamma$ and WWH could induce an enhancement of the Branching ratio (Br) expected for the two-photon decay mode of the SM Higgs boson [4, 5]. This topic has been the subject of renewed interest after the recent announcement of the discovery of a new neutral scalar boson, first hinted by CDF and D0 in a wide mass interval between 115 and 130 GeV or so [6], then finally confirmed with a mass of 125.2 $\pm 0.3 \pm 0.6$ GeV and $125.8 \pm 0.4 \pm 0.4$ GeV by the ATLAS and CMS Collaborations, respectively [7, 8]. The new particle seen at

the Fermi National Accelerator Laboratory (FNAL) and Large Hadron Collider (LHC) is presently rather compatible with the neutral Higgs boson of the SM [9–11]. However, this is not a certainty and the LHC will aim at establishing once and forever whether such an object is really the Higgs particle of the SM (or not) during its upcoming runs [12, 13]. In fact, following the initial discovery announcement on 4^{th} July 2012, there has been much speculation about the excess of events in the decay channel $h \to \gamma\gamma$ initially suggested by both ATLAS and CMS [7, 8], though more recently CMS (but not ATLAS) have claimed an opposite effect [14, 15]. This potential excess could be explained by the existence of additional charged particles running in the loops of the radiative Higgs coupling to photons, how it happens in some extended Higgs sectors [16–34]. Conversely, if this enhancement in $h \to \gamma\gamma$ disappears, it will still constrain the parameter space of various extensions of the SM. Another decay channel that is closely related to the di-photon one and that might give another clean signal in the LHC experiments is the γZ mode, wherein the same new charged particles would contribute [35]. Despite being highly suppressed processes, the $h \to \gamma\gamma$ and $h \to \gamma Z$ decays, for the above reason, can nonetheless offer a window of understanding into possible Beyond the SM (BSM) scenarios even when no new states are found in real processes. In particular, the simultaneous measurement of these channels at the LHC will (eventually) provide us with significant information about the possible underlying structure of the Higgs sector, as in most BSM scenarios the rates of these two channels scale (almost identically, in most cases) with respect to the SM ones [21, 36, 37]. The upcoming higher-energy LHC run, which is expected to start in 2015 at $\sqrt{s} \approx 13 - 14\,\text{TeV}$ with $100\,\text{fb}^{-1}$ of luminosity per year, will greatly extend the experimental sensitivity to BSM physics, irrespectively of whether it is produced through real or virtual dynamics. Furthermore, one of many currently discussed e^+e^- facilities, like the International Linear Collider (ILC) [38], the Compact Linear Collider (CLIC) [39] and the Triple Large Electron-Positron (TLEP) collider [40], may be commissioned within a decade or so, thereby offering the possibility of carrying out high precision Higgs analyses. Therefore, it is very timely to study the scope of the $\gamma\gamma$ and γZ signatures in disentangling a possible non-minimal structure of the Higgs sector.

In this paper, we address the potential, in the above respect, of the most general version of a Two Higgs Doublet Model which is of Type III (2HDM-III), wherein the fermionic couplings of the ensuing neutral scalars are non-diagonal in flavor and the Higgs potential is the most general one compatible with Electro-Weak Symmetry Breaking (EWSB) (and CP conservation). This framework, however, potentially embeds unwanted Flavor Changing Neutral Current (FCNC) phenomena [41]. The simplest and most common approach to avoid these is to impose a $\mathcal{Z}_2$ symmetry forbidding all non-diagonal terms in flavor space in the model Lagrangian [42]. Herein, we focus instead on the version where the Yukawa couplings depend on the hierarchy of masses. This construct is the one where the mass matrix has a four-zero texture form [43, 44] forcing the non-diagonal Yukawa couplings to be proportional to the geometric mean of the two fermion masses involved [45–49]. This matrix is based on the phenomenological observation that the off-diagonal elements have to be small in order to dim the interactions that violate flavor, as innumerable experimental results show.

JHEP07(2014)057

In the next section, we briefly describe the theoretical structure of the Yukawa sector in the 2HDM-III. In section III, we present the Feynman rules for the $\gamma\gamma\phi$ and for $\gamma Z\phi$ interactions (where ϕ signifies the intervening Higgs boson, either CP-even or CP-odd). In section IV, we present our numerical results. In section V, we summarize and conclude. Finally, some more technical details of the calculations are relegated to the appendix.

2 The Higgs-Yukawa sector of the 2HDM-III

The 2HDM includes two Higgs scalar doublets of hypercharge +1: $\Phi_1^\dagger = (\phi_1^-, \phi_1^{0*})$ and $\Phi_2^\dagger = (\phi_2^-, \phi_2^{0*})$. The most general $\mathrm{SU}(2)_L \times \mathrm{U}(1)_Y$ invariant scalar potential can be written as [50]

$$\begin{aligned} V(\Phi_1,\Phi_2) = {} & \mu_1^2(\Phi_1^\dagger\Phi_1) + \mu_2^2(\Phi_2^\dagger\Phi_2) - \Big(\mu_{12}^2(\Phi_1^\dagger\Phi_2) + \mathrm{H.c.}\Big) + \frac{1}{2}\lambda_1(\Phi_1^\dagger\Phi_1)^2 \\ & + \frac{1}{2}\lambda_2(\Phi_2^\dagger\Phi_2)^2 + \lambda_3(\Phi_1^\dagger\Phi_1)(\Phi_2^\dagger\Phi_2) + \lambda_4(\Phi_1^\dagger\Phi_2)(\Phi_2^\dagger\Phi_1) \\ & + \left(\frac{1}{2}\lambda_5(\Phi_1^\dagger\Phi_2)^2 + \Big(\lambda_6(\Phi_1^\dagger\Phi_1) + \lambda_7(\Phi_2^\dagger\Phi_2)\Big)(\Phi_1^\dagger\Phi_2) + \mathrm{H.c.}\right), \end{aligned} \tag{2.1}$$

where all parameters are assumed to be real, including the scalar field vacuum expectation values $\langle\Phi\rangle_1^\dagger = (0, v_1)$ and $\langle\Phi\rangle_2^\dagger = (0, v_2)$, namely, both explicit and spontaneous CP-violation do not occur.[1] When a specific four-zero texture is implemented as a flavor symmetry in the Yukawa sector, discrete symmetries in the Higgs potential are not needed. Hence, one must keep the terms proportional to λ_6 and λ_7. These parameters play an important role in one-loop processes though, where self-interactions of Higgs bosons could be relevant [51]. In particular, with our assumptions, the Higgs potential is not invariant under the so-called custodial symmetryl $\mathrm{SU}(2)_L \times \mathrm{SU}(2)_R$ only when $\lambda_4 \neq \lambda_5$ [41, 52]. Then, the possibility of large contributions to the $\rho = m_W^2/m_Z^2\cos^2\theta_W$ parameter comes only from the difference $(\lambda_4 - \lambda_5)$, which can be rewritten in terms of $(m_{H^\pm}^2 - m_A^2)$, being large. In ref. [50], we can get the general expression of the Higgs spectrum and one obtains in particular the squared mass for the charged Higgs state:

$$m_{H^\pm}^2 = m_A^2 + \frac{1}{2}v^2(\lambda_4 - \lambda_5). \tag{2.2}$$

Recently, another possibility was studied in ref. [53], where a twisted custodial symmetry is presented and generalizes the case above. This symmetry is broken when $m_{H^\pm} - m_A$ or $m_{H^\pm} - m_H$ are sizable. In both cases, we must also consider the corresponding mass of the CP-even neutral Higgs H-state:

$$m_H^2 = m_A^2 + v^2\left(\lambda - \lambda_A + \hat{\lambda}\frac{\cos(\beta-\alpha)}{\sin(\beta-\alpha)}\right), \tag{2.3}$$

where the parameters λ, λ_A and $\hat{\lambda}$ are given in ref. [50] and are functions of all parameters λ_i. Following the analysis of this reference, we can get in the SM-like scenario ($\cos(\beta-\alpha) \to$

[1] The μ_{12}^2, λ_5, λ_6 and λ_7 parameters are complex in general, but we will assume that they are real for simplicity.

JHEP07(2014)057

0) that $(m_A^2 - m_H^2) = \mathcal{O}(v^2)$ and, using eq. (2.2), we can also relate $m_{H^\pm} - m_H$ to the difference $(\lambda_4 - \lambda_5)$. Consequently, the parameters λ_6 and λ_7 are not so relevant in the contributions to the ρ parameter. Besides, the twisted symmetry allows for a scenario where the pseudoscalar Higgs state is light [41, 54], which will be discussed below. As the Higgs potential has CP-conservation, one can avoid mixing among the real and imaginary parts of the neutral scalar fields, so that the general expressions of the oblique parameters are reduced to those given in ref. [55].[2] Although the parameters λ_6 and λ_7 can avoid to be constrained by the ρ parameter, there are other ways to subject them to various tests, e.g., perturbativity and unitarity [41]. In particular, we found that the strongest constraint for the most general Higgs potential of the 2HDM comes from tree-level unitarity [58]. We found numerically the following constraint for $\tan\beta \leq 10$:

$$|\lambda_{6,7}| \leq 1, \tag{2.4}$$

which will be used in all our subsequent work.

In order to derive the interactions of the type Higgs-fermion-fermion, the Yukawa Lagrangian is written as follows:

$$\mathcal{L}_Y = -\Big(Y_1^u \bar{Q}_L \tilde{\Phi}_1 u_R + Y_2^u \bar{Q}_L \tilde{\Phi}_2 u_R + Y_1^d \bar{Q}_L \Phi_1 d_R + Y_2^d \bar{Q}_L \Phi_2 d_R + Y_1^l \bar{L}_L \Phi_1 l_R + Y_2^l \bar{L}_L \Phi_2 l_R\Big), \tag{2.5}$$

where $\Phi_{1,2} = (\phi_{1,2}^+, \phi_{1,2}^0)^T$ refer to the two Higgs doublets, $\tilde{\Phi}_{1,2} = i\sigma_2 \Phi_{1,2}^*$. After spontaneous EWSB, one can derive the fermion mass matrices from eq. (2.5), namely: $M_f = \frac{1}{\sqrt{2}}(v_1 Y_1^f + v_2 Y_2^f)$, $f = u,\ d,\ l$, assuming that both Yukawa matrices Y_1^f and Y_2^f have the four-texture form and are Hermitian [47–49]. The diagonalisation is performed in the following way: $\bar{M}_f = V_{fL}^\dagger M_f V_{fR}$. Then, $\bar{M}_f = \frac{1}{\sqrt{2}}(v_1 \tilde{Y}_1^f + v_2 \tilde{Y}_2^f)$, where $\tilde{Y}_i^f = V_{fL}^\dagger Y_i^f V_{fR}$. One can derive a better approximation for the product $V_q\, Y_n^q\, V_q^\dagger$, by expressing the rotated matrix $\tilde{Y}_n^q$ as

$$\left[\tilde{Y}_n^q\right]_{ij} = \frac{\sqrt{m_i^q m_j^q}}{v}\,[\tilde{\chi}_n^q]_{ij} = \frac{\sqrt{m_i^q m_j^q}}{v}\,[\chi_n^q]_{ij}\; e^{i\vartheta_{ij}^q}, \tag{2.6}$$

where the χ's are unknown dimensionless parameters of the model. Following the recent analysis of [59, 60] (see also [61]), we can obtain the generic expression for the interactions of the Higgs bosons with the fermions,

$$\begin{aligned}\mathcal{L}^{\bar{f}_i f_j \phi} = &-\left\{\frac{\sqrt{2}}{v}\bar{u}_i\left(m_{d_j} X_{ij} P_R + m_{u_i} Y_{ij} P_L\right) d_j\, H^+ + \frac{\sqrt{2} m_{l_j}}{v} Z_{ij} \overline{\nu_L} l_R H^+ + H.c.\right\} \\ &-\frac{1}{v}\left\{\bar{f}_i m_{f_i} h_{ij}^f f_j h^0 + \bar{f}_i m_{f_i} H_{ij}^f f_j H^0 - i\bar{f}_i m_{f_i} A_{ij}^f f_j \gamma_5 A^0\right\},\end{aligned} \tag{2.7}$$

where ϕ_{ij}^f ($\phi = h,\ H,\ A$), X_{ij}, Y_{ij} and Z_{ij} are defined as follows:

$$\phi_{ij}^f = \xi_\phi^f \delta_{ij} + G(\xi_\phi^f, X), \quad \phi = h, H, A, \tag{2.8}$$

[2] When the most general Higgs potential with CP-violation is considered, one must use the general expressions of the oblique parameters given in [56, 57].

JHEP07(2014)057

2HDM-III	X	Y	Z	ξ_h^u	ξ_h^d	ξ_h^l	ξ_H^u	ξ_H^d	ξ_H^l
2HDM-I-like	$-\cot\beta$	$\cot\beta$	$-\cot\beta$	c_α/s_β	c_α/s_β	c_α/s_β	s_α/s_β	s_α/s_β	s_α/s_β
2HDM-II-like	$\tan\beta$	$\cot\beta$	$\tan\beta$	c_α/s_β	$-s_\alpha/c_\beta$	$-s_\alpha/c_\beta$	s_α/s_β	c_α/c_β	c_α/c_β
2HDM-X-like	$-\cot\beta$	$\cot\beta$	$\tan\beta$	c_α/s_β	c_α/s_β	$-s_\alpha/c_\beta$	s_α/s_β	s_α/s_β	c_α/c_β
2HDM-Y-like	$\tan\beta$	$\cot\beta$	$-\cot\beta$	c_α/s_β	$-s_\alpha/c_\beta$	c_α/s_β	s_α/s_β	c_α/c_β	s_α/s_β

Table 1. Parameters ξ_ϕ^f, X, Y and Z defined in the Yukawa interactions of eqs. (5)–(8) for four versions of the 2HDM-III with a four-zero texture. Here $s_\alpha = \sin\alpha$, $c_\alpha = \cos\alpha$, $s_\beta = \sin\beta$ and $c_\beta = \cos\beta$.

$$X_{ij} = \sum_{l=1}^{3}(V_{\rm CKM})_{il}\left[X\,\frac{m_{d_l}}{m_{d_j}}\,\delta_{lj} - \frac{f(X)}{\sqrt{2}}\,\sqrt{\frac{m_{d_l}}{m_{d_j}}}\,\tilde{\chi}^d_{lj}\right], \tag{2.9}$$

$$Y_{ij} = \sum_{l=1}^{3}\left[Y\,\delta_{il} - \frac{f(Y)}{\sqrt{2}}\,\sqrt{\frac{m_{u_l}}{m_{u_i}}}\,\tilde{\chi}^u_{il}\right](V_{\rm CKM})_{lj}, \tag{2.10}$$

$$Z^l_{ij} = \left[Z\,\frac{m_{l_i}}{m_{l_j}}\,\delta_{ij} - \frac{f(Z)}{\sqrt{2}}\,\sqrt{\frac{m_{l_i}}{m_{l_j}}}\,\tilde{\chi}^l_{ij}\right], \tag{2.11}$$

where $G(\xi_\phi^f, X)$ and $f(x)$ can be obtained from [59, 60] and the parameters ξ_ϕ^f, X, Y and Z are given in the table 1. When the parameters $\chi_{ij}^f = 0$, one recovers the Yukawa interactions given in refs. [62–64]. As it was pointed out in [59, 60], we suggest that this Lagrangian could also represent a Multi-Higgs Doublet Model (MHDM) or an Aligned 2HDM (A2HDM) with additional flavor physics in the Yukawa matrices as well as the possibility of FCNCs at tree level. Here, we present our analysis for the four versions of the 2HDM-III with a four-zero texture introduced in the aforementioned table.

3 Feynman rules

In this section we present the Higgs sector Lagrangian which describes the $\gamma\gamma\phi$ and $\gamma Z\phi$ vertices. First, we write the general effective Lagrangian through first order (i.e., at one-loop level in perturbation theory). Then, we will show the explicit form factors in the 2HDM-III.

The effective Lagrangian can be written as following way:

$$\mathcal{L}_{\phi\gamma V} = \frac{1}{4}\Delta_{1\gamma\gamma}\phi_a F_{\mu\nu}F^{\mu\nu} + \frac{1}{4}\Delta_{2\gamma\gamma}A F_{\mu\nu}\widetilde{F}^{\mu\nu} + \Delta_{1\gamma Z}\phi_a F_{\mu\nu}\partial^\mu Z^\nu + \Delta_{2\gamma Z}A\widetilde{F}_{\mu\nu}\partial^\mu Z^\nu, \tag{3.1}$$

where ϕ_a $(a = 1, 2)$ is any neutral Higgs boson, with CP-even parity, predicted by the model. Similarly, the A represents the neutral Higgs boson with CP-odd parity. Further, $F^{\mu\nu}$ and $\widetilde{F}^{\mu\nu}$ are the electromagnetic tensor and the dual tensor, respectively. The definitions for these tensors are:

$$F^{\mu\nu} = \partial^\mu A^\nu - \partial^\nu A^\mu, \tag{3.2}$$

$$\widetilde{F}^{\mu\nu} = \frac{1}{2}\epsilon^{\mu\nu\alpha\beta}F_{\alpha\beta}. \tag{3.3}$$

JHEP07(2014)057

Now, using the Lagrangian which has been presented in eq. (3.1), the Feynman rules for $\gamma\gamma\phi$ and $\gamma Z\phi$ ($\phi = \phi_a, A$) can be written as:

$$g_{\phi_a\gamma\gamma} = i\Delta_{1\gamma\gamma}(k_1^\nu k_2^\mu - k_1\cdot k_2 g^{\mu\nu}), \tag{3.4}$$

$$g_{A\gamma\gamma} = i\Delta_{2\gamma\gamma}\epsilon^{\mu\nu\alpha\beta}k_{1\alpha}k_{2\beta}, \tag{3.5}$$

$$g_{\phi_a\gamma Z} = i\Delta_{1\gamma Z}(k_1^\nu k_2^\mu - k_1\cdot k_2 g^{\mu\nu}), \tag{3.6}$$

$$g_{A\gamma Z} = i\Delta_{2\gamma Z}\epsilon^{\mu\nu\alpha\beta}k_{1\alpha}k_{2\beta}, \tag{3.7}$$

where the $\Delta_{j\gamma V}$ (with $j = 1{,}2$ and $V = Z,\ \gamma$) represent the form factors for the one-loop couplings. The scheme of momentum is k_1^μ for a photon and k_2^ν for the second photon or the Z boson. Finally, the tensor amplitudes are obtained from eqs. (3.4)–(3.7) and these can be written in terms of the CP-even and CP-odd parts,

$$\mathcal{M}^{\mu\nu}_{\text{even}} = i\Delta_{1\gamma V}(k_1^\nu k_2^\mu - k_1\cdot k_2 g^{\mu\nu}), \tag{3.8}$$

$$\mathcal{M}^{\mu\nu}_{\text{odd}} = i\Delta_{2\gamma V}\epsilon^{\mu\nu\alpha\beta}k_{1\alpha}k_{2\beta}, \tag{3.9}$$

Now, the decay $\Gamma(\phi_i \to \gamma V)$ can be completely determined considering the explicit forms of $\Delta_{i\gamma V}$ for the 2HDM-III which are presented in the two upcoming subsections where we have introduced the following notation: $V = \gamma, Z$ and $i = 1, 2$ with $i = 1$ for ϕ_a (which in turn refers to either h or H) and $i = 2$ for A. The explicit expressions for the two decays studied are shown in appendix A.

3.1 Form factor $\Delta_{1\gamma\gamma}$

Here, we present the explicit expressions for the $\Delta_{i\gamma\gamma}$ form factor in the 2HDM-III. This form factor receives contributions from all charged particles, for this reason it is convenient to separate each sector:

$$\Delta_{1\gamma\gamma} = \Delta^0_{1\gamma\gamma} + \Delta^1_{1\gamma\gamma} + \Delta^{1/2}_{1\gamma\gamma}. \tag{3.10}$$

In the last equation we have labelled with 0 the contribution from the scalar sector, with 1/2 from the fermionic sector and with 1 from the gauge sector. In an explicit way, these contributions are (refer to figure 1):

$$\Delta^0_{1\gamma\gamma} = \frac{-\alpha^{3/2}m_W}{4\pi^{1/2}s_W k_1\cdot k_2}\Big[2m^2_{H^\pm}C_0(1,2)+1\Big]\mathcal{G}_{\phi_i H^\pm H^\mp}, \tag{3.11}$$

$$\Delta^1_{1\gamma\gamma} = \frac{-\alpha^{3/2}}{\pi^{1/2}m_W s_W k_1\cdot k_2}\Big[6m^2_W(m^2_W - k_1\cdot k_2)C_0(1,2) + k_1\cdot k_2 + 3m^2_W\Big]\mathcal{G}_{\phi_i WW}, \tag{3.12}$$

$$\Delta^{1/2}_{1\gamma\gamma} = \sum_f \frac{2\alpha^{3/2}N_c m_f^2 Q_f^2}{\pi^{1/2}m_W s_W k_1\cdot k_2}\Big[(2m_f^2 - k_1\cdot k_2)C_0(1,2)+1\Big]\mathcal{G}_{\phi_a\bar{f}f}. \tag{3.13}$$

Here, we have introduced two shorthand notations. The first is $\mathcal{G}_{ABC}$, which represents the dimensionless function related to the couplings between the particles ABC (see appendix B). The second shorthand notation is for the Passarino-Veltman functions, that is

$$C_0(a,b) = C_0(k_a^2, k_b^2, 2k_a\cdot k_b, m^2, m^2, m^2), \tag{3.14}$$

where m^2 has to be taken according to every particle in the loop.

JHEP07(2014)057

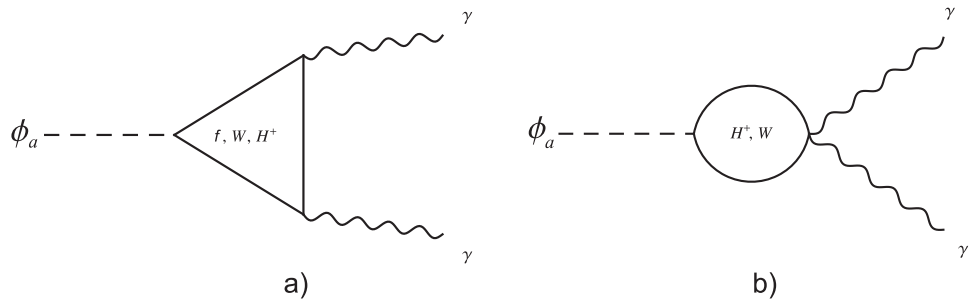

Figure 1. The Feynman diagrams for the $\phi_a\gamma\gamma$ vertex.

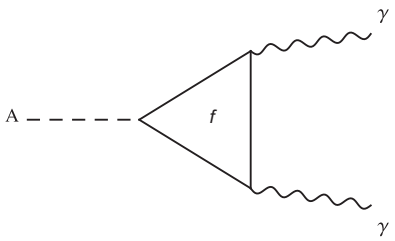

Figure 2. The Feynman diagram for the $A\gamma\gamma$ vertex.

3.2 Form factor $\Delta_{2\gamma\gamma}$

This form factor, due to the presence of a Higgs boson A, only receives contributions from the fermionic sector. These contributions are introduced through the Feynman diagram shown in figure 2. The explicit expression for this form factor is:

$$\Delta_{2\gamma\gamma} = \sum_f \frac{-4ie^3 N_c m_f^2 Q_f^2}{m_W s_W} C_0(1,2)\mathcal{G}_{A\bar{f}f}. \tag{3.15}$$

3.3 Form factor $\Delta_{1\gamma Z}$

Now, for the $\gamma Z\phi_a$ vertex, we will have again contributions from all charged particles, see figure 3. Therefore, it is again convenient to separate every contribution. Hence, we have

$$\begin{aligned}\Delta^0_{1\gamma Z} =& \frac{-m_W\alpha^{3/2}c_{2W}}{8\pi^{1/2}s_W s_{2W}(k_1\cdot k_2)^2}\Big\{k_1\cdot k_2\Big[4m^2_{H^\pm}C_0(1,2)+2\Big]\\ &+m_Z^2\Big[B_0(P)-B_0(k_2)\Big]\Big\}\mathcal{G}_{\phi H^\pm H^\mp},\end{aligned} \tag{3.16}$$

$$\begin{aligned}\Delta^1_{1\gamma Z} =& \frac{-c_W\alpha^{3/2}}{8\pi^{1/2}m_W^3 s_W^2(k_1\cdot k_2)^2}\mathcal{G}_{\phi_a WW}\Big\{4C_0(1,2)m_W^2 k_1\cdot k_2\Big[2(k_2^2-6m_W^2)k_1\cdot k_2\\ &-k_2^2+12m_W^4\Big]-\Big[(2k_2^2-4m_W^2)k_1\cdot k_2+k_2^2-12m_W^4\Big]\\ &\times(k_2^2[B_0(P)-B_0(k_2)]+2k_1\cdot k_2)\Big\},\end{aligned} \tag{3.17}$$

$$\begin{aligned}\Delta^{1/2}_{1\gamma Z} =& \sum_f \frac{f_V N_c m_f^2 Q_f \alpha^{3/2}}{4\pi^{1/2}c_W s_W^2 m_W(k_1\cdot k_2)^2}\Big\{2k_1\cdot k_2\Big[(2m_f^2-k_1\cdot k_2)C_0(1,2)+1\Big]\\ &+m_Z^2\Big[B_0(P)-B_0(k_2)\Big]\Big\}\mathcal{G}_{\phi ff}.\end{aligned} \tag{3.18}$$

JHEP07(2014)057

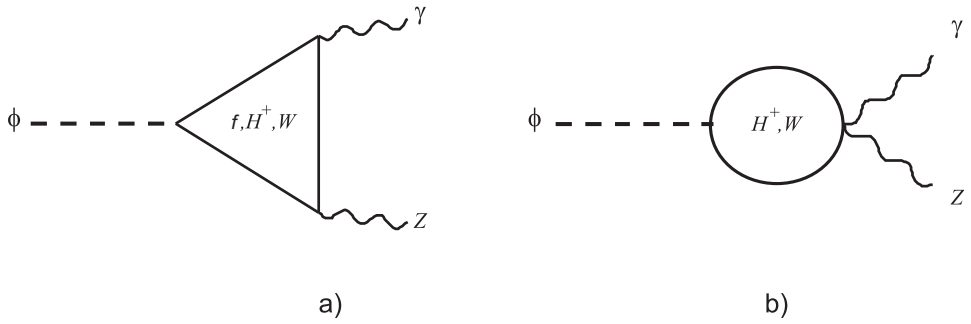

Figure 3. The Feynman diagrams for the $\phi Z\gamma$ vertex.

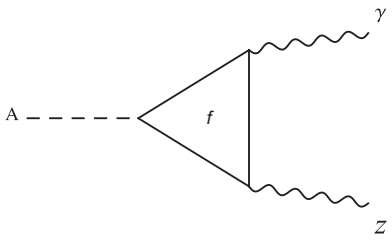

Figure 4. The Feynman diagram for the $AZ\gamma$ vertex.

Here, f_V is the vector part of the coupling $\bar{f}fZ$ (see its explicit form in appendix B). Also, we have used a shorthand notation for the B_0 Passarino-Veltman function, this is

$$B_0(k) = B_0(k \cdot k, m^2, m^2). \tag{3.19}$$

3.4 Form factor $\Delta_{2\gamma Z}$

For this case, similarly to $\Delta_{2\gamma\gamma}$, the form factor receives contributions only from the fermionic sector, see figure 4. Explicitly, we can write as follows:

$$\Delta_{2\gamma Z} = \sum_f \frac{-ie^3 f_V m_f^2 Q_f N_c}{c_W s_W^2 m_W} C(1,2)\mathcal{G}_{A\bar{f}f}. \tag{3.20}$$

4 Discussion

In this section we will present the results for the two Brs of interest, i.e., of the channels $\phi \to \gamma\gamma$ and γZ, where (again) $\phi = \phi_a$ or A. Recently, some of us have studied the flavor constraints affecting the 2HDM-III and we have isolated the surviving parameter space [59, 60] (again, see also [61]), which we are going to re-use in our present analysis. Besides, we will incorporate an extensive discussion of the most popular models, like 2HDM-I, 2HDM-II, 2HDM-X and 2HDM-Y, which are particular incarnations of our 2HDM-III. However, do recall that experimental results suggest a SM-like Higgs signal, for this reason we have therefore chosen the following scenario

$$\beta - \alpha = \frac{\pi}{2} + \delta, \tag{4.1}$$

JHEP07(2014)057

$$\lambda_6 = -\lambda_7, \tag{4.2}$$

$$\mu_{12} \sim v, \tag{4.3}$$

where δ is considered near to zero and where we take $\mu_{12} = 200\,\text{GeV}$. Besides, we can observe that is more convenient to use $\lambda_6 = -\lambda_7$ instead of $\lambda_6 = \lambda_7$ because the rates of $h \to \gamma\gamma$, γZ can receive the greatest enhancement. In the opposite case, $\lambda_6 = \lambda_7$, the contribution to the decay is irrelevant (see the three Higgs bosons vertices Feynman rules of appendix B). So that our settings naturally comply with the SM-like scenario advocated in ref. [50].

4.1 The $h \to \gamma\gamma$, γZ decays

In this section we present the results for the case of h decays. We start with a general discussion of all decay channels and we finally comment on the two specific channels of interest. In the left panel of figure 5, where the $h \to AA$ decay is forbidden, one can see that the behavior of all decay channels is similar to the SM case [65]. However, if the decay $h \to AA$ is kinetically allowed (see right panel), all SM channels show a strong reduction, as this mode becomes dominant for most m_h values. For this special case ($m_A < m_h/2$), there is a small region of parameter space of our model, where this channel decay is allowed. Following the study of new physics effects on the electroweak oblique parameters parametrized by S, T and U [55], we find for $2m_A < m_h$ and $m_H \sim 200$ - $230\,\text{GeV}$, taking $\sin(\beta - \alpha) \sim 1$, the range allowed for the charged Higgs boson mass is given by $150\,\text{GeV} \leq m_{H^\pm} \leq 200\,\text{GeV}$. Using these values for the masses of neutral and charged Higgs bosons, we can confront the parameter space of our model with the main flavor physics constraints, which are studied in [59, 60, 66]. We can obtain practically the same constraints for the parameters of Yukawa matrices with a four-zero texture, except for the off-diagonal term, χ^d_{23}, which must be very tiny and it has the following bound $|\chi^d_{23}| \leq 10^{-1}$. The process $B_s \to \mu^+\mu^-$ imposes the most strong constraint to the parameter χ^d_{23} (see the formula of this process in the refs. [59, 60]). On the other hand, we should consider another assumption, the possibility to observe this channel decay at LHC. In ref. [67] the decay $h \to AA$ is studied in a model-independent way with $2m_A < (m_h - 10)\,\text{GeV}$, this channel could provide sizable significances for an integrated luminosity $L = 30\ fb^{-1}$ and adequate b-tagging efficiencies. Therefore, if we want to have a h boson that be SM-like, we have to demand that $2m_A > m_h$, so that the decay $h \to AA$ is forbidden. For reference, hereafter, we are using the 2HDM-III Like II (for reasons which will become clear below).

As we can see in figure 6, the $\text{Br}(h \to \gamma\gamma)$ is very sensitive to the X parameter given in eq. (2.9). For large values of the latter, in particular, the $\text{Br}(h \to \gamma\gamma)$ shows an enhancement of one order of magnitude, but this behavior is contrary to the experimental results from the LHC. In contrast, for medium values of X (say, $X < 15$), this increase is under control, indeed compatible with the LHC data, so that we will choose a definite value in this range, e.g., $X = 10$, from now on. We will instead change the values of other parameters, like the mass of the charged Higgs boson, m_{H^+}.

JHEP07(2014)057

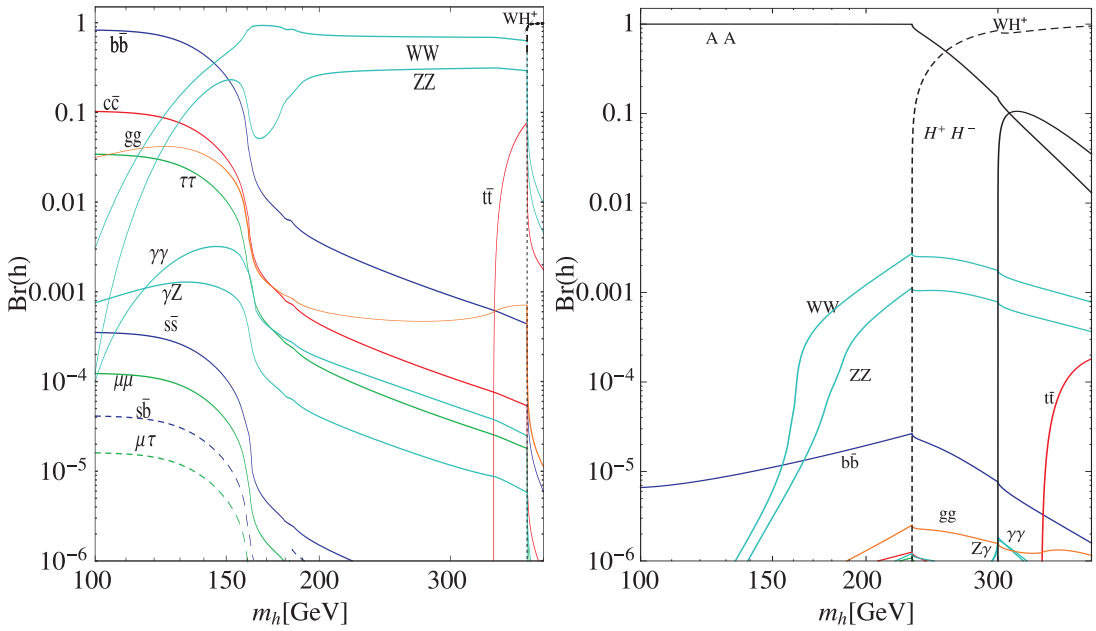

Figure 5. Behavior of all decay channels of the light CP-even Higgs boson h with respect to its mass for the 2HDM-III Like II. The parameters used are as follows: $\chi^u_{kk} = \chi^d_{kk} = 1$, $\chi^u_{23} = -0.75$, $\lambda_7 = -\lambda_6 = -1$, $X = 10$ for (a) $m_A > m_h$, $m_{H^+} = 300\,\text{GeV}$ and $\chi^d_{23} = -0.035$ (left panel) and (b) $m_A = 40\,\text{GeV}$, $m_{H^+} = 150\,\text{GeV}$ and $\chi^d_{23} = 0.002$ (right panel).

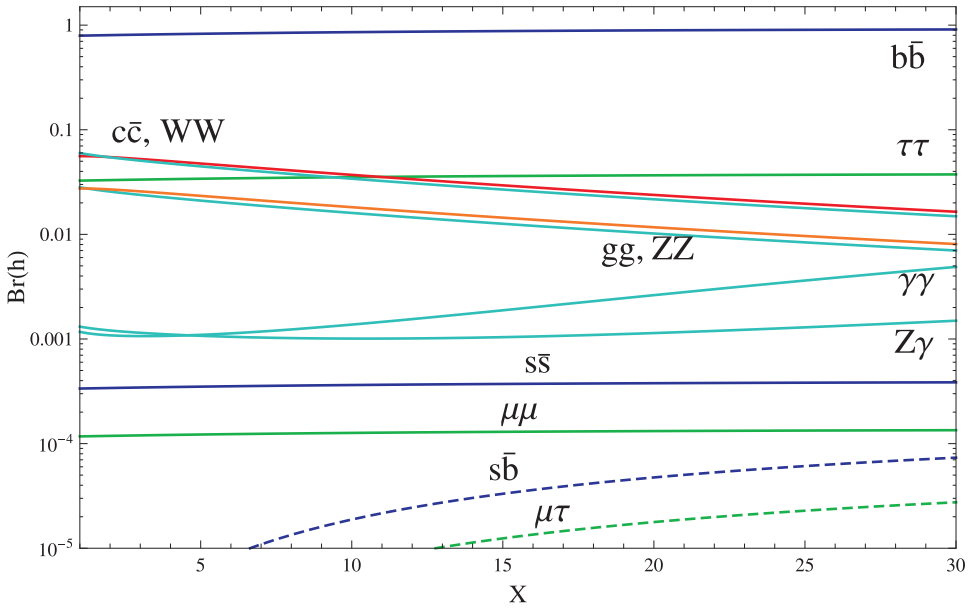

Figure 6. Behavior of all decay channels of the light CP-even Higgs boson h with respect to the X parameter of eq. (2.9) for the 2HDM-III Like II. The other parameters are the same as in the left frame of figure 5.

JHEP07(2014)057

In the remainder of this subsection, we analyze $h \to \gamma\gamma$ and γZ relative to the SM case, by introducing the so-called R parameters,

$$R_{\gamma X} = \frac{\sigma(gg \to h)|_{\text{2HDM-III}} \times \text{Br}(h \to \gamma X)|_{\text{2HDM-III}}}{\sigma(gg \to h)|_{\text{SM}} \times \text{Br}(h \to \gamma X)|_{\text{SM}}} \approx \mathcal{G}_{htt}^2 \frac{\text{Br}(h \to \gamma X)|_{\text{2HDM-III}}}{\text{Br}(h \to \gamma X)|_{\text{SM}}} \ (X = \gamma, Z), \tag{4.4}$$

where $\mathcal{G}_{htt}$ is the ratio of the couplings $htt|_{\text{2HDM-III}}$ and $htt|_{\text{SM}}$ entering the hgg effective vertex (see appendix A). Notice that, in the case of a fermiophobic h state, the $gg \to h$ production mode ought to be replaced by either vector boson fusion or Higgs-strahlung, for which the ratio of cross sections reduces to unity, so that the above formula remains applicable upon the replacement $\mathcal{G}_{htt} \to 1$.

In figure 7 we show the behavior of $R_{\gamma\gamma}$ and $R_{\gamma Z}$ with respect to the charged Higgs boson mass, m_{H^+}. In the plots, the shaded areas represent the fits to the experimental results from the LHC. In particular, the scenarios presented are the following: the black line is for an exactly SM-like h state ($\delta = 0$), the red line represents the case when the Yukawa couplings are equal to the 2HDM with $\mathcal{Z}_2$ symmetry, the blue line is associated to a set of Yukawa couplings with FCNCs ($\chi^d_{23} = -0.35$ and $\chi^u_{23} = -0.75$), finally, the green line illustrates the fermiophobic scenario.

One can see in the figure that the most relevant scenarios are: 2HDM-III-like II and Y with $\chi^f_{kk} = 0$ and the fermiophobic scenario for 2HDM-III-like I, II and Y. The parameterisations 2HDM-III-like X is disadvantaged for all scenarios presented. The fermiophobic scenario demands a charged Higgs boson very light, between 80 and 90 GeV for the 2HDM-like I, II and Y. Notice that the $\chi^f_{kk} = 0$ scenario opens up the possibility of a light charged Higgs boson, $m_{H^+} \geq 110\,\text{GeV}$, for 2HDM-III-like II and Y, as already seen in [59, 60].

Because the most important signatures are generated into the context of the 2HDM-III-like II and Y, from now on we are going to systematically focus on 2HDM-III-like II. Within this scenario, we present in figure 8 the allowed parameter space (after enforcing the LHC constraints) mapped onto the $m_{H^+} - X$ plane, for two values of $\lambda_{6,7}$ and a definite choice of δ (here, $X = \tan\beta$: see table 1). As we can see, the final state γZ is the most constrained one, in the sense that LHC results are reproduced in a smaller region of parameters with respect to the case of $\gamma\gamma$. In particular, the former decay demands a mass of the charged Higgs boson below ≈ 160 GeV for $X = 20$ and $\lambda_7 = -\lambda_6 = -0.1$ and below 230 GeV for $\lambda_7 = -\lambda_6 = -1$. This is a valuable result, as charged Higgs bosons with such a mass and with $X = 20$ are indeed accessible at the LHC (albeit at high energy and luminosity only). In fact, for more acceptable values of X which are mid-range, e.g. around 15, we find that $m_{H^+} < m_t$, so that this state is copiously produced in top quark decays. Again, as already emphasized in refs. [59, 60], a light charged Higgs boson could be a hallmark manifestation of a 2HDM-III.

Finally, in the graphics presented in figure 9, we map the same parameter space described by the previous plot now in terms of the plane (m_{H^+} , $\lambda_7 = -\lambda_6$). As we can see, when $\lambda_{6,7} = 0$, the overlapping areas required by the decays $h \to \gamma\gamma$ and γZ suggest a H^+ mass around $100 - 150\,\text{GeV}$, however, for $\lambda_7 = -\lambda_6 = -1$, the limit for this mass goes up

JHEP07(2014)057

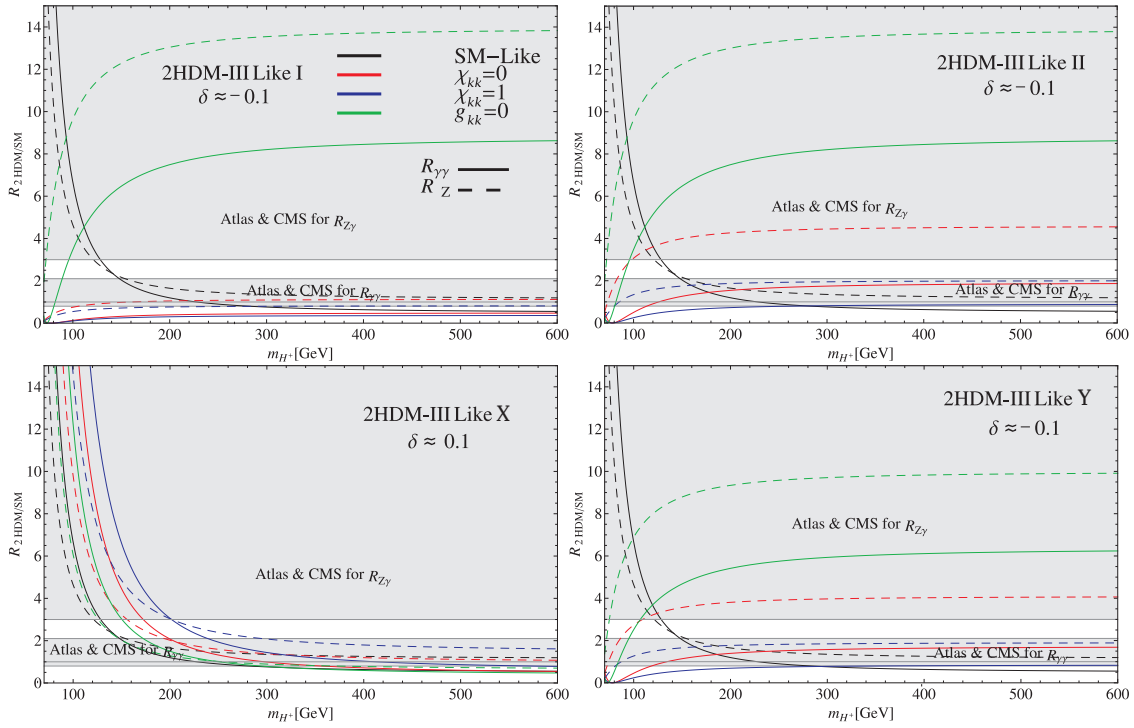

Figure 7. $R_{\gamma\gamma}$ (solid-line) and $R_{\gamma Z}$ (dashes-line) with respect to the charged Higgs boson mass. In all cases $\lambda_7 = -\lambda_6 = -1$. The other parameters are given in the legends and described in the text.

to 160 GeV, in line with our previous findings. Besides, we show in the yellow area region excluded by tree-level unitarity.

4.2 The $H \to \gamma\gamma$, γZ decays

In this subsection, we present the results for the Brs of the heavy CP-even Higgs state, denoted by H. We present them only for the case of the 2HDM-III Like II, because this scenario allows for the existence of a light charged Higgs boson ($m_{H^+} \sim 100$ GeV), a key signature of this scenario which will be accessible at the LHC, as previously explained.

In figure 10 we present all the decay channels of the heavy Higgs state. Herein, as we can see, Higgs-to-Higgs decays can again be dominant, whenever $m_H > 2m_h, 2m_A, 2m_{H^+}$, as the channels $H \to hh, AA, H^+H^-$ overwhelm all others. However, in the m_H region where these channels are forbidden, the final states $\gamma\gamma$ and γZ turn out to be very important, becoming order of 10^{-1}, a significant increase above and beyond the SM rates, and only second in size to the $H \to b\bar{b}$ mode.

Next, we present the results for the Br($H \to \gamma\gamma$) and Br($H \to \gamma Z$) versus the heavy Higgs boson mass for three different values of the charged Higgs boson one (see figure 11). The scenarios presented in these plots are: the fermiophobic one ($g_{kk} = 0$), the one with Yukawa couplings mimicking a $\mathcal{Z}_2$ symmetry ($\chi^f_{kk} = 0$) and a general 2HDM. Before the $H \to hh$ decay is allowed, the differences between these scenarios are relevant, about two orders of magnitude (this between $g_{kk} = 0$ and $\chi^f_{kk} = 0$ at $m_{H^+} = 200$ GeV). However,

JHEP07(2014)057

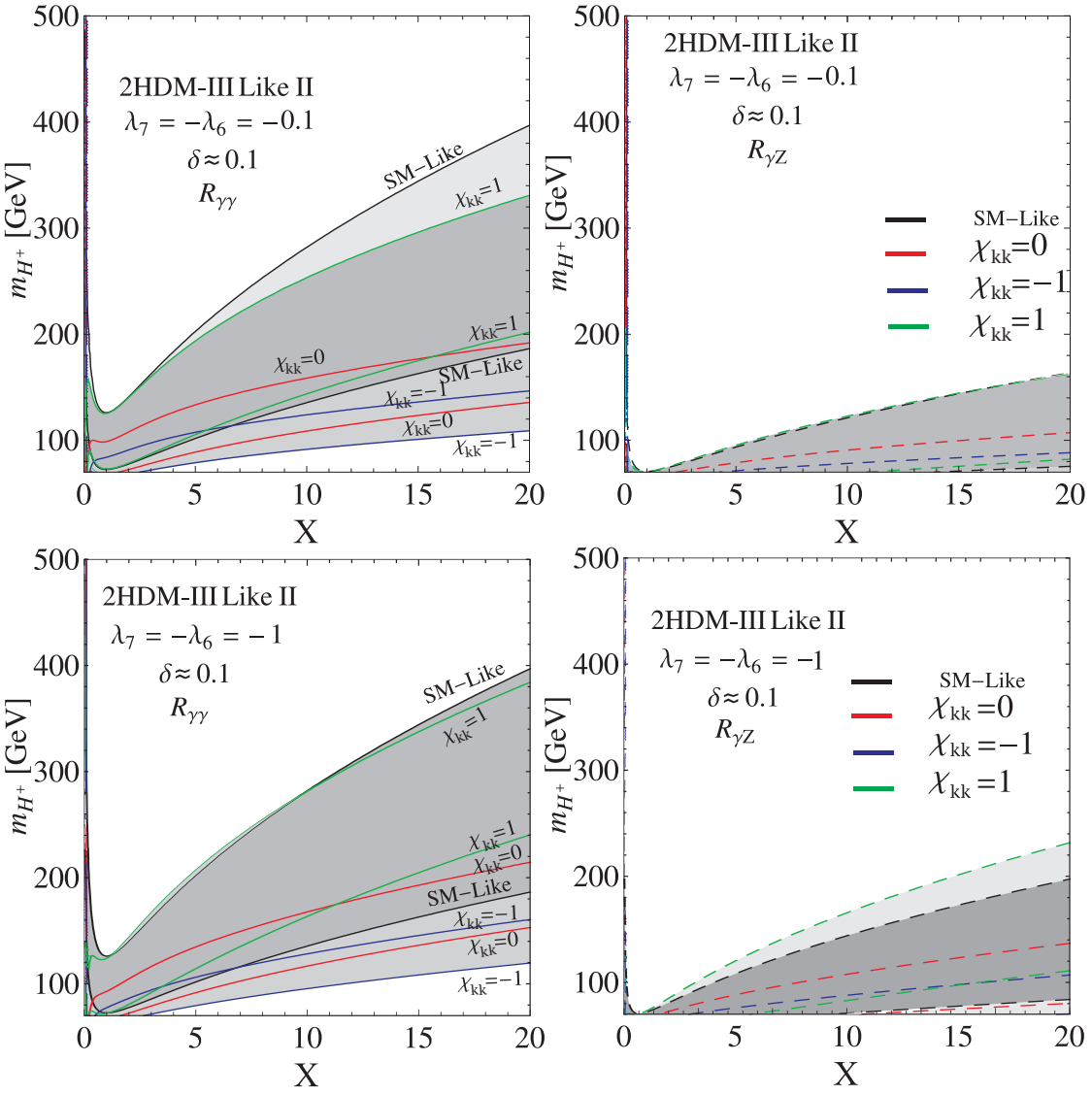

Figure 8. Constraints over the $(m_{H^+},\ X \equiv \tan\beta)$ parameter space of the 2HDM-III-like II derived from $R_{\gamma\gamma}$ (solid-line) and $R_{\gamma Z}$ (dashes-line) measurements at the LHC (the shaded areas and enclosed by lines of the same color, are the allowed permitted region by CMS and ATLAS). The values of $\lambda_{6,7}$ and δ are given in the legends.

when a light charged Higgs boson mass is considered ($m_{H^+} = 100\,\text{GeV}$), the scenarios $\chi^f_{kk} = 0$ and $\chi^f_{kk} = 1$ yield similar rates for the $\gamma\gamma$ and γZ decay channels, both with Brs around 10^{-1}. Finally, the $\text{Br}(H \to \gamma\gamma)$ and $\text{Br}(H \to \gamma Z)$ are disadvantaged when the heavy Higgs boson mass allows for the channels $H \to hh, AA$ or H^+H^- to be open as, after this happens, these loop decays are reduced to below the 10^{-5} level.

4.3 The $A \to \gamma\gamma$, γZ decays

In this last result subsection, we illustrate the decay phenomenology of the CP-odd Higgs boson, denoted by A. We start our discussion with figure 12, where we present the behavior

JHEP07(2014)057

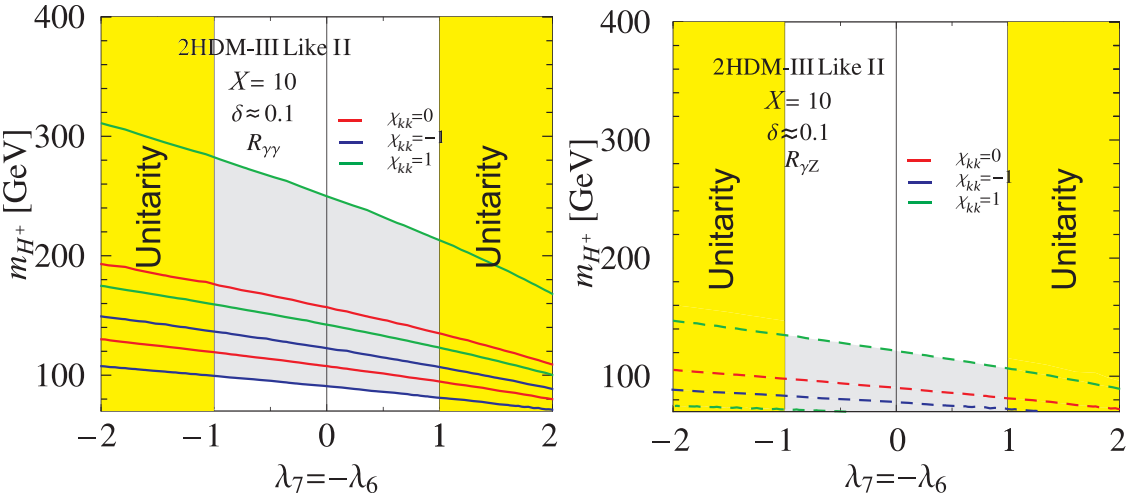

Figure 9. Constraints over the $(m_{H^+}, \lambda_7 = -\lambda_6)$ parameter space of the 2HDM-III-like II derived from $R_{\gamma\gamma}$ (solid-line) and $R_{\gamma Z}$ (dashes-line). Again, the shaded areas and enclosed by lines of the same color, are the allowed region by LHC. The yellow region is not allowed by constraints of tree-level unitarity

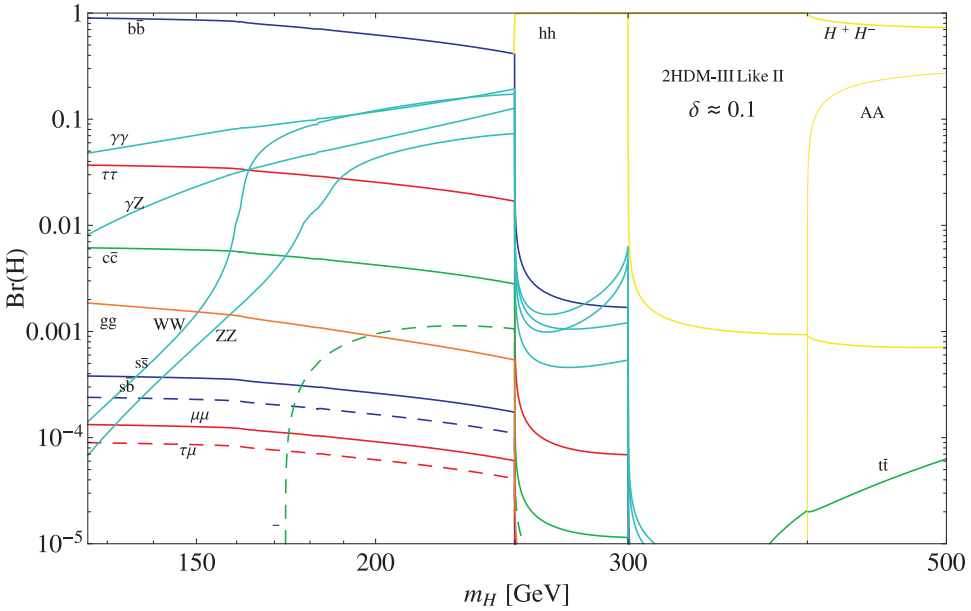

Figure 10. Behavior of all decay channels of the heavy CP-even Higgs boson H with respect to its mass for the 2HDM-III Like II. The parameters used are as follows: $m_A = 200\,\text{GeV}$, $m_{H^+} = 150\,\text{GeV}$, $\lambda_7 = -\lambda_6 = -1$, $\chi^f_{kk} = 1$, $\chi^f_{23} = -0.35$, $\chi^u_{23} = -0.75$ and $X = 10$.

JHEP07(2014)057

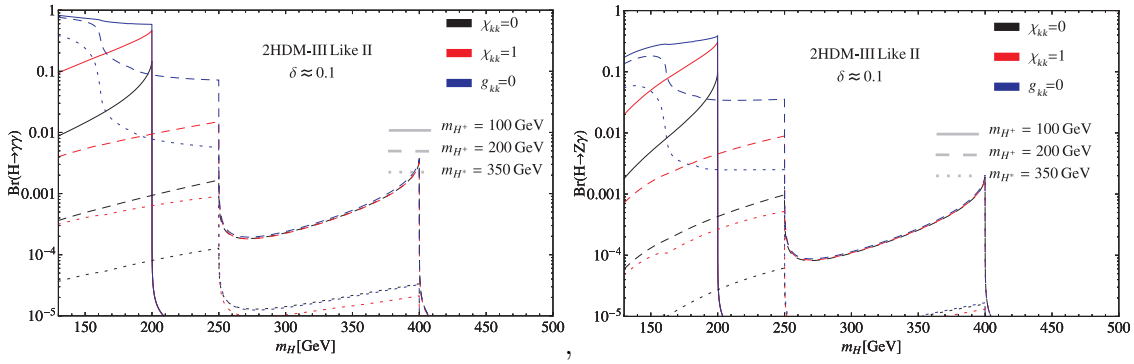

Figure 11. Decay rates for the channels $H \to \gamma\gamma$ (left frame) and $H \to \gamma Z$ (right frame) versus the heavy CP-even Higgs mass for the 2HDM-III Like II. The parameters used here are as follows: $m_A = 200\,\text{GeV}$, $\lambda_7 = -\lambda_6 = -1$, $\chi^f_{kk} = 1$, $\chi^d_{23} = -0.35$, $\chi^u_{23} = -0.75$ and $X = 10$.

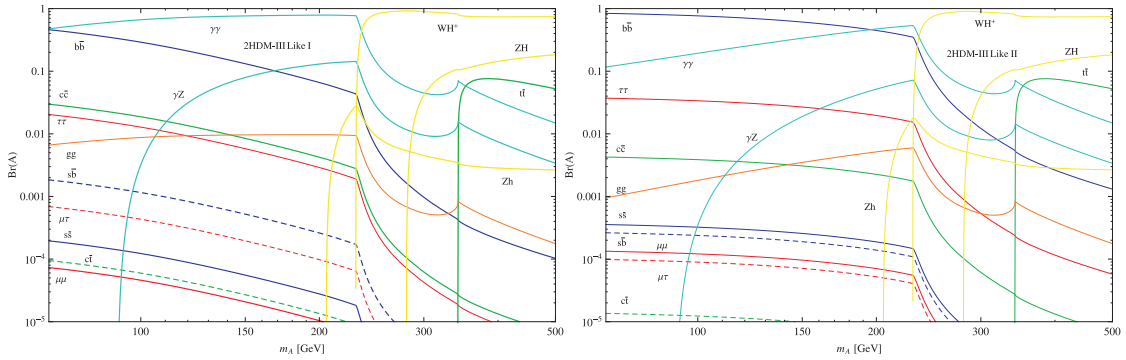

Figure 12. Behavior of all decay channels of the CP-odd Higgs boson A with respect to its mass for the 2HDM-III-like I (left frame) and 2HDM-III-like II (right frame). The parameters used are as follows: $m_H = 200\,\text{GeV}$, $m_{H^+} = 150\,\text{GeV}$, $\lambda_7 = -\lambda_6 = -1$, $\chi^f_{kk} = 1$, $\chi^d_{23} = -0.35$, $\chi^u_{23} = -0.75$ and $X = 10$.

of all decay channels in the context of the 2HDM-III-like I and II. The coupling Aff presents high sensitivity to the underlying model, since while for the 2HDM-III-like I case it is proportional to $\cot\beta$ and for the 2HDM-III-like II it is proportional to $\tan\beta$. On the one hand, for the case of the 2HDM-III-like I (left plot) the most relevant decay is $A \to \gamma\gamma$ as the $A \to b\bar{b}$ decay rate is reduced by a factor of $1/10$ (as we have considered the choice $X = \tan\beta = 10$). On the other hand, in the 2HDM-III-like II context (right plot) the relevant decay is $A \to b\bar{b}$ for the opposite reason (for large $\tan\beta$). However, even in this last case the decay $A \to \gamma\gamma$ presents a size which is relevant, as $\text{Br}(A \to \gamma\gamma) \sim 10^{-1}$. In general, when the m_A value is large enough to allow for the decays to WH^+, Zh or ZH, the channels $A \to \gamma\gamma$ and γZ are reduced by an order of magnitude. However, this pair of channels continue to be relevant.

In figure 13 we present the $\text{Br}(A \to \gamma\gamma)$ and $\text{Br}(A \to \gamma Z)$ versus the A boson mass and for three different values of m_{H^+}. Unlike the previous CP-even states, for the case of the CP-odd Higgs boson it is impossible to implement a fermiophobic scenario, because only the fermionic particles contribute to the loops. For this reason, we can see that the

JHEP07(2014)057

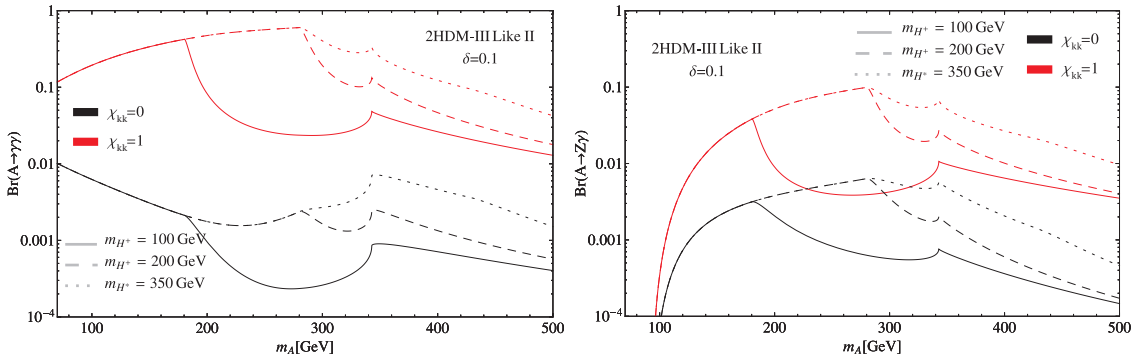

Figure 13. Decay rates for the channels $A \to \gamma\gamma$ (left frame) and $A \to \gamma Z$ (right frame) versus the CP-odd Higgs mass for the 2HDM-III-like II. The parameters used here are as follows: $m_H = 200\ GeV$, $\lambda_7 = -\lambda_6 = -1$, $\chi^f_{kk} = 1$, $\chi^d_{23} = -0.35$, $\chi^u_{23} = -0.75$ and $X = 10$.

difference between the two scenarios $\chi^f_{kk} = 1$ and $\chi^f_{kk} = 0$ can be up to two orders of magnitude. The most relevant results are achieved via the $\chi^f_{kk} = 1$ scenario, yielding a Br of $\mathcal{O}(10^{-1})$ for $\gamma\gamma$ and of $\mathcal{O}(10^{-2})$ for γZ. In the same plots, again, it can be observed the strong sensitivity to the channels $A \to H^+W, hZ$ and HZ since, once these channels are open, the loop BRs decrease by about an order of magnitude.

5 Conclusions

We have studied the significant enhancement of the Brs of the decay channels $h \to \gamma\gamma$ and $h \to \gamma Z$ in the context of the 2HDM-III, assuming a four-zero Yukawa texture and a general Higgs potential. We have shown that these processes are very sensitive to the flavor structure represented by such a Yukawa texture and to the triple Higgs couplings entering the Lagrangian of the scalar sector. We also have shown that it is possible to accommodate the parameters of the model in such a way to obtain the decay $h \to \gamma\gamma$ rates reported by the LHC and we have found a decay rate for $h \to \gamma Z$ up to one order of magnitude larger than that one obtained in the SM, hence amenable to experimental investigation with current and/or future LHC data. We have then presented some benchmarks where the parameters of the scenario considered are consistent with all current experimental constraints. In addition, we have found that it is possible to have a light charged Higgs boson compatible with all such measurements too, thereby serving the purpose of being the smoking gun signal of the model considered, particularly in its Like II incarnation. We can finally confirm that the aforementioned loop decays can be enhanced, with respect to the corresponding SM rates, also for the case of the heavy Higgs state H while for the A one (which has no SM counterpart). The corresponding rates can be sizable in certain regions of the 2HDM-III Like II parameter space for both Higgs states as well as the 2HDM-III Like I for the latter only. We finally note that the scaling of the $\gamma\gamma$ and γZ rates with respect to the corresponding ones in the SM is not the same, unlike the case of many other BSM scenarios, thereby offering an alternative means to extract evidence of the most general 2HDM-III considered here.

JHEP07(2014)057

Acknowledgments

This work has been supported in part by *SNI-CONACYT (México)* and by *PROMEP (México)* under the grant "Red Temática: Física del Higgs y del sabor". SM is financed in part through the NExT Institute. He is also grateful for the hospitality extended to him by the Benemérita Universidad Autónoma de Puebla, where part of this work was carried out.

A Higgs bosons tree level decays

In this appendix we present explicitly the decay formulae for the neutral Higgs states of the 2HDM-III at tree level [68–72]. Notice that these have been written according to the notation used in this work.

A.1 Decay into fermions pairs

We first present the decay of a neutral Higgs boson to pairs of fermions, without FCNCs (like in the SM and the standard 2HDM with a $\mathcal{Z}_2$ symmetry). These decays can be written as follows:

$$\Gamma(\phi_i \to f\bar{f}) = \frac{N_c m_\phi}{8\pi}\left(\frac{g m_f}{2m_W}\right)^2\left(1-\frac{4m_f^2}{m_\phi^2}\right)^{\rho/2}\mathcal{G}^2_{\phi f\bar{f}}, \tag{A.1}$$

where $\rho = 3$ if $\phi = h, H$ and $\rho = 1$ for $\phi = A$. However, in the 2HDM-III it is indeed possible to have FCNCs, so that it is important to know the corresponding decays, whichever their size, which are:

$$\begin{aligned}\Gamma(\phi \to f_i\bar{f}_j) = {} & \frac{N_c}{8\pi m_\phi}\left(\frac{g m_i}{2m_W}\right)^2\left[m_\phi^2-(m_i+(-1)^n m_j)^2\right] \\ & \times\sqrt{\left[1-\left(\frac{m_i-m_j}{m_\phi}\right)^2\right]\left[1-\left(\frac{m_i+m_j}{m_\phi}\right)^2\right]}\,\mathcal{G}^2_{\phi f_i\bar{f}_j},\end{aligned} \tag{A.2}$$

here $n = 0$ for a Higgs boson which is CP-even and $n = 1$ for the CP-odd state.

A.2 Decay into vector particles

One more possibility is that Higgs particles decay into two real gauge bosons. These decay channels can be written as

$$\Gamma(\phi_a \to VV) = \frac{G_f m_\phi^3}{16\sqrt{2}\pi}\delta_V\sqrt{1-4x}(1-4x+12x^2)\mathcal{G}^2_{\phi VV}, \quad V=\{Z,W\}, \tag{A.3}$$

where G_f is the Fermi constant, $x = m_V^2/m_\phi^2$ and $\delta_W = 2$ and $\delta_Z = 1$. Another option is to have one virtual gauge boson, for this case the partial width is

$$\begin{aligned}\Gamma(\phi_a \to VV^*) = {} & \frac{3G_f^2 M_V^4}{16\pi^3}m_\phi\delta'\left[\frac{3(1-8x+20x^2)}{(4x-1)^{1/2}}\arccos\left(\frac{3x-1}{2x^{3/2}}\right)\right. \\ & \left.-\frac{1-x}{2x}(2-13x+47x^2)-\frac{3}{2}(1-6x+4x^2)\log x\right]\mathcal{G}^2_{\phi VV},\end{aligned} \tag{A.4}$$

with $\delta'_W = 1$ and $\delta'_Z = \frac{7}{12}-\frac{10}{9}s_W^2+\frac{40}{9}s_W^4$.

With respect to the CP-odd state, A, there are two channels:

$$\Gamma(A \to WH^+) = \frac{g[(m_W^2 + m_{H^+}^2 - m_A^2) - 4m_{H^+}^2 m_W^2]^{3/2}}{16 m_A^3 m_W^2 \pi}, \tag{A.5}$$

$$\Gamma(A \to Z\phi) = \frac{g^2[(m_Z^2 + m_\phi^2 - m_A^2)^2 - 4m_\phi^2 m_Z^2]^{3/2}}{64\pi m_Z^2 m_A^3 c_W^2} \mathcal{G}_\phi^2, \tag{A.6}$$

with $\mathcal{G}_h = c_{\beta-\alpha}$, and $\mathcal{G}_H = s_{\beta-\alpha}$.

A.3 Decay into gluons

Now we present the decay into pairs of gluons. We begin with decays for the CP-even Higgs bosons:

$$\Gamma(\phi \to gg) = \frac{\alpha_s^2 g^2 m_\phi^2}{128\pi^3 m_W^2} \left| \sum_q \tau_q [1 + (1-\tau_q) f(\tau_q)] \right|^2 g_{\phi ff}^2, \tag{A.7}$$

where $\tau_q = 4m_q^2/m_\phi^2$ and

$$f_(\tau_q) = \begin{cases} \arcsin(\sqrt{1/\tau_q})^2 & if\ \tau_q \geq 1, \\ \frac{1}{4}[\log(\eta_+/\eta_-) - i\pi]^2 & if\ \tau_q < 1, \end{cases} \tag{A.8}$$

with $\eta_\pm = (1 \pm \sqrt{1-\tau_q})$. For the CP-odd state, A, we have instead:

$$\Gamma(A \to gg) = \frac{\alpha_s^2 g^2 m_A^3}{128\pi^3 m_W^2} \left| \sum_q \tau_q f(\tau_q) \right|^2 \mathcal{G}_{Aff}^2. \tag{A.9}$$

A.4 Decay into Higgs bosons

Finally, the possibility of Higgs-to-Higgs decays is presented in this subsection. We start with the widths for pairs of neutral Higgs bosons:

$$\Gamma(\phi \to AA) = \frac{\mathcal{G}_{\phi AA}^2}{32 m_\phi^2 \pi} \sqrt{m_\phi^2 - 4m_A^2}, \tag{A.10}$$

$$\Gamma(H \to hh) = \frac{\mathcal{G}_{Hhh}^2}{32 m_H^2 \pi} \sqrt{m_H^2 - 4m_h^2}, \tag{A.11}$$

with

$$\begin{aligned} \mathcal{G}_{hAA} = \frac{-g}{8m_W} \Bigg\{ & 8m_A^2 s_{\beta-\alpha} + 2m_h^2 \frac{c_{\alpha-3\beta} + 3c_{\beta+\alpha}}{s_{2\beta}} - 2m_{H^+}^2 \left(\frac{c_\alpha}{c_\beta} - 1 \right) (s_{\alpha+3\beta} - 3s_{\beta-\alpha}) \\ & -16\mu_{12}^2 \frac{c_{\beta+\alpha}}{s_{2\beta}^2} + \frac{8m_W^2 c_{\beta-\alpha}}{g^2} \left(\frac{\lambda_6}{s_\beta^2} - \frac{\lambda_7}{c_\beta^2} \right) \Bigg\}, \end{aligned} \tag{A.12}$$

$$\begin{aligned} \mathcal{G}_{HAA} = \frac{-g}{8m_W} \Bigg\{ & 8m_A^2 c_{\beta-\alpha} + 2m_H^2 \frac{s_{\alpha-3\beta} + 3s_{\beta+\alpha}}{s_{2\beta}} + 2m_{H^+}^2 \left(\frac{c_\alpha}{c_\beta} - 1 \right) (c_{\alpha+3\beta} + 3s_{\beta-\alpha}) \\ & -16\mu_{12}^2 \frac{s_{\beta+\alpha}}{s_{2\beta}^2} - \frac{8m_W^2 s_{\beta-\alpha}}{g^2} \left(\frac{\lambda_6}{s_\beta^2} - \frac{\lambda_7}{c_\beta^2} \right) \Bigg\}, \end{aligned} \tag{A.13}$$

JHEP07(2014)057

$\mathcal{G}_{\phi_i ff}$	leptons	quarks-down	quarks-up
h	$\xi_h^l\delta_{ij}+\frac{\xi_H^l-Z\xi_h^l}{\sqrt{2}f(Z)}\sqrt{\frac{m_{l_j}}{m_{l_i}}}\chi_{ij}^l$	$\xi_h^d\delta_{ij}+\frac{\xi_H^d-X\xi_h^d}{\sqrt{2}f(X)}\sqrt{\frac{m_{d_j}}{m_{d_i}}}\chi_{ij}^d$	$\xi_h^u\delta_{ij}-\frac{\xi_H^u+Y\xi_h^u}{\sqrt{2}f(Y)}\sqrt{\frac{m_{u_j}}{m_{u_i}}}\chi_{ij}^u$
H	$\xi_H^l\delta_{ij}-\frac{\xi_h^l-Z\xi_H^l}{\sqrt{2}f(Z)}\sqrt{\frac{m_{l_j}}{m_{l_i}}}\chi_{ij}^l$	$\xi_H^d\delta_{ij}-\frac{\xi_h^d-X\xi_H^d}{\sqrt{2}f(X)}\sqrt{\frac{m_{d_j}}{m_{d_i}}}\chi_{ij}^d$	$\xi_H^u\delta_{ij}+\frac{\xi_h^u+Y\xi_H^u}{\sqrt{2}f(Y)}\sqrt{\frac{m_{u_j}}{m_{u_i}}}\chi_{ij}^u$
A	$-Z\delta_{ij}+\frac{f(Z)}{\sqrt{2}}\sqrt{\frac{m_{l_j}}{m_{l_i}}}\chi_{ij}^l$	$-X\delta_{ij}+\frac{f(X)}{\sqrt{2}}\sqrt{\frac{m_{d_j}}{m_{d_i}}}\chi_{ij}^d$	$-Y\delta_{ij}+\frac{f(Y)}{\sqrt{2}}\sqrt{\frac{m_{u_j}}{m_{u_i}}}\chi_{ij}^u$

Table 2. Dimensionless functions that define the Yukawa couplings in the 2HDM-III.

$$\mathcal{G}_{Hhh}=\frac{-gc_{\beta-\alpha}}{2m_W s_{2\beta}^2}\Big\{(2m_h^2+m_H^2)s_{2\alpha}s_{2\beta}+2\mu_{12}^2(s_{2\beta}-3s_{2\alpha}) \\ +\frac{12m_W^2 s_{2(\alpha-\beta)}}{g^2}(\lambda_6 c_\beta^2-\lambda_7 s_\beta^2)\Big\}. \tag{A.14}$$

Finally, the width for $H\to H^+H^-$ can be written as follows:

$$\Gamma(H\to H^+H^-)=\frac{g^2\mathcal{G}_{HH^+H^-}^2 m_W^2}{256m_H^2\pi}\sqrt{m_H^2-4m_{H^+}^2}. \tag{A.15}$$

B Couplings

In this section we present all the couplings that we have used for this work. These will be presented in general form, together with the explicit factors for every scenario.

B.1 Fermion couplings

We begin with the Yukawa couplings, which have already appeared in section II of this work. In a general way, these couplings are:

$$g_{\phi_a ff} = \frac{-igm_f}{2m_W}\mathcal{G}_{\phi_a ff}, \tag{B.1}$$

$$g_{Aff} = \frac{gm_f}{2m_W}\gamma^5\mathcal{G}_{Aff}, \tag{B.2}$$

where the factors $\mathcal{G}$ are defined in table 2.

Others couplings needed for this work are the vector-fermion-fermion couplings. Essentially, for this analysis we need $\gamma f\bar{f}$ and $Zf\bar{f}$, which are described as

$$g_{\gamma ff} = -ieQ_f\gamma_\mu, \tag{B.3}$$

$$g_{Zff} = \frac{ig}{4c_W}\gamma_\mu(F_V-F_A\gamma_5), \tag{B.4}$$

where, $F_V(F_A)$ represents the vectorial(axial) part of the couplings and their explicit form is shown in table 3.

JHEP07(2014)057

	for u-quarks	for d-quarks	for leptons
F_V	$1-\frac{8}{3}s_W^2$	$1+\frac{4}{3}s_W^2$	$-1+4s_W^2$
F_A	-1	1	1

Table 3. Axial and vector components for the $Z\bar{f}f$ couplings.

Coupling	Vertex Function	Coupling	Vertex Function
$g_{\phi_i H^\pm H^\mp}$	$\frac{-igm_W}{4}\mathcal{G}_{\phi_i H^\pm H^\mp}$	$g_{\phi_a WW}$	$igm_W\mathcal{G}_{\phi_a WW}g_{\mu\nu}$
$g_{\gamma H^\pm H^\mp}$	$ie(P_- - P_+)_\mu$	$g_{ZH^\pm H^\mp}$	$iet_{2W}^{-1}(P_- - P_+)_\mu$
$g_{\gamma\gamma H^\pm H^\mp}$	$2ie^2 g_{\mu\nu}$	$g_{Z\gamma H^\pm H^\mp}$	$2ie^2 t_{2W}^{-1}g_{\mu\nu}$

Table 4. The three- and four-particle couplings between scalars and vectors in the 2HDM-III.

B.2 Gauge sector

Now, we write the couplings for the gauge sector. For this calculation it is convenient to adopt the unitary gauge, so that the couplings $V^\mu(k_1)W^{+\lambda}(k_2)W^{-\rho}(k_3)$ and $V_1^\mu V_2^\nu W^{+\lambda}W^{-\rho}$ (where the V^μs represent any neutral vector boson) can be written as $ig_V\Gamma_{\lambda\rho\mu(k_1,k_2,k_3)}$ and $ig_{V_1}g_{V_2}\Gamma_{\lambda\rho\mu\nu}$, with

$$\Gamma_{\lambda\rho\mu}(k_1,k_2,k_3) = (k_2-k_3)_\mu g_{\lambda\rho} + \Big(k_3-k_1\Big)_\lambda g_{\rho\mu} + \Big(k_1-k_2\Big)_\rho g_{\lambda\mu}, \tag{B.5}$$

$$\Gamma_{\lambda\rho\mu\nu} = -2g_{\mu\nu}g_{\lambda\rho} + g_{\lambda\mu}g_{\rho\nu} + g_{\rho\mu}g_{\lambda\nu}, \tag{B.6}$$

$g_\gamma = gs_W$ and $g_Z = gc_W$.

B.3 Scalar and kinetic sector

Finally, the couplings between scalar particles themselves and scalar-vector-vector couplings are presented in table 4. Herein, we have $\mathcal{G}_{hWW} = s_{\beta-\alpha}$ ($\mathcal{G}_{HWW} = c_{\beta-\alpha}$) and

$$\begin{aligned}\mathcal{G}_{hH^+H^-} = \frac{-1}{16g^2m_W^2}\Bigg\{&16g^2\mu_{12}^2\frac{c_{\alpha+\beta}}{s_{2\beta}^2} + \frac{g^2m_{H^+}^2}{c_\beta}\Big(s_{\alpha-2\beta}+3s_{2\alpha-\beta}-s_{\alpha+2\beta}+s_{2\alpha+3\beta}\\ &-s_{\alpha+4\beta}+s_\alpha-3s_\beta+s_{3\beta}\Big) - 2g^2m_h^2\frac{c_{\alpha-3\beta}+3c_{\alpha+\beta}}{s_{2\beta}} - 8m_W^2\lambda_6\frac{c_{\alpha-\beta}}{s_\beta^2}\\ &+8m_W^2\lambda_7\frac{c_{\alpha-\beta}}{c_\beta^2}\Bigg\},\end{aligned} \tag{B.7}$$

$$\begin{aligned}\mathcal{G}_{HH^+H^-} = \frac{-1}{16g^2m_W^2}\Bigg\{&16g^2\mu_{12}^2\frac{s_{\alpha+\beta}}{s_{2\beta}^2} - \frac{g^2m_{H^+}^2}{c_\beta}\Big(c_{\alpha-2\beta}+3c_{2\alpha-\beta}-c_{\alpha+2\beta}+c_{2\alpha+3\beta}\\ &-c_{\alpha+4\beta}+c_\alpha+3c_\beta+c_{3\beta}\Big) - 2g^2m_H^2\frac{s_{\alpha-3\beta}+3s_{\alpha+\beta}}{s_{2\beta}} - 8m_W^2\lambda_6\frac{s_{\alpha-\beta}}{s_\beta^2}\\ &+8m_W^2\lambda_7\frac{s_{\alpha-\beta}}{c_\beta^2}\Bigg\}.\end{aligned} \tag{B.8}$$

JHEP07(2014)057

References

[1] R. Martinez, M.A. Perez and J.J. Toscano, *The Two Photon Decay Width of the Higgs Boson in Left-right Symmetric Theories*, *Phys. Rev.* **D 40** (1989) 1722 [INSPIRE].

[2] R. Martinez, M.A. Perez and J.J. Toscano, *The Decays $H^0 \to Z\gamma$ and $Z' \to H^0\gamma$ in Left-right Symmetric Models*, *Phys. Lett.* **B 234** (1990) 503 [INSPIRE].

[3] J. Wudka, *Electroweak effective Lagrangians*, *Int. J. Mod. Phys.* **A 9** (1994) 2301 [hep-ph/9406205] [INSPIRE].

[4] M.A. Perez and J.J. Toscano, *The Decay $H^0 \to \gamma\gamma$ and the nonstandard couplings $WW\gamma$, WWH*, *Phys. Lett.* **B 289** (1992) 381 [INSPIRE].

[5] J.M. Hernandez, M.A. Perez and J.J. Toscano, *Decays $H^0 \to \gamma\gamma$, γZ, and $Z \to \gamma H^0$ in the effective Lagrangian approach*, *Phys. Rev.* **D 51** (1995) 2044 [INSPIRE].

[6] CDF, D0 collaboration, T. Aaltonen et al., *Evidence for a particle produced in association with weak bosons and decaying to a bottom-antibottom quark pair in Higgs boson searches at the Tevatron*, *Phys. Rev. Lett.* **109** (2012) 071804 [arXiv:1207.6436] [INSPIRE].

[7] ATLAS collaboration, *Observation of a new particle in the search for the Standard Model Higgs boson with the ATLAS detector at the LHC*, *Phys. Lett.* **B 716** (2012) 1 [arXiv:1207.7214] [INSPIRE].

[8] CMS collaboration, *Observation of a new boson at a mass of 125 GeV with the CMS experiment at the LHC*, *Phys. Lett.* **B 716** (2012) 30 [arXiv:1207.7235] [INSPIRE].

[9] S.L. Glashow, *Partial Symmetries of Weak Interactions*, *Nucl. Phys.* **22** (1961) 579.

[10] S. Weinberg, *A Model of Leptons*, *Phys. Rev. Lett.* **19** (1967) 1264 [INSPIRE].

[11] A. Salam, *Weak and Electromagnetic Interactions*, *Conf. Proc.* **C 680519** (1968) 367.

[12] A. Djouadi, *The Anatomy of electro-weak symmetry breaking. I: The Higgs boson in the standard model*, *Phys. Rept.* **457** (2008) 1 [hep-ph/0503172] [INSPIRE].

[13] A. Djouadi, *Implications of the Higgs discovery for the MSSM*, *Eur. Phys. J.* **C 74** (2014) 2704 [arXiv:1311.0720] [INSPIRE].

[14] ATLAS collaboration, *Combined measurements of the mass and signal strength of the Higgs-like boson with the ATLAS detector using up to 25 fb^{-1} of proton-proton collision data*, ATLAS-CONF-2013-014 (2013).

[15] CMS collaboration, *CMS Collaboration*, CMS-PAS-HIG-13-005 (2013).

[16] P.M. Ferreira, R. Santos, M. Sher and J.P. Silva, *Could the LHC two-photon signal correspond to the heavier scalar in two-Higgs-doublet models?*, *Phys. Rev.* **D 85** (2012) 035020 [arXiv:1201.0019] [INSPIRE].

[17] P.M. Ferreira, R. Santos, M. Sher and J.P. Silva, *Implications of the LHC two-photon signal for two-Higgs-doublet models*, *Phys. Rev.* **D 85** (2012) 077703 [arXiv:1112.3277] [INSPIRE].

[18] S. Kanemura and K. Yagyu, *Radiative corrections to electroweak parameters in the Higgs triplet model and implication with the recent Higgs boson searches*, *Phys. Rev.* **D 85** (2012) 115009 [arXiv:1201.6287] [INSPIRE].

[19] T. Kitahara, *Vacuum Stability Constraints on the Enhancement of the $h \to \gamma\gamma$ rate in the MSSM*, *JHEP* **11** (2012) 021 [arXiv:1208.4792] [INSPIRE].

JHEP07(2014)057

[20] A. Delgado, G. Nardini and M. Quirós, *Large diphoton Higgs rates from supersymmetric triplets*, *Phys. Rev.* **D 86** (2012) 115010 [arXiv:1207.6596] [INSPIRE].

[21] C.-W. Chiang and K. Yagyu, *Higgs boson decays to $\gamma\gamma$ and $Z\gamma$ in models with Higgs extensions*, *Phys. Rev.* **D 87** (2013) 033003 [arXiv:1207.1065] [INSPIRE].

[22] D.S.M. Alves, P.J. Fox and N.J. Weiner, *Higgs Signals in a Type I 2HDM or with a Sister Higgs*, arXiv:1207.5499 [INSPIRE].

[23] N. Craig and S. Thomas, *Exclusive Signals of an Extended Higgs Sector*, *JHEP* **11** (2012) 083 [arXiv:1207.4835] [INSPIRE].

[24] W. Altmannshofer, S. Gori and G.D. Kribs, *A Minimal Flavor Violating 2HDM at the LHC*, *Phys. Rev.* **D 86** (2012) 115009 [arXiv:1210.2465] [INSPIRE].

[25] L. Basso, A. Lipniacka, F. Mahmoudi, S. Moretti, P. Osland et al., *Probing the charged Higgs boson at the LHC in the CP-violating type-II 2HDM*, *JHEP* **11** (2012) 011 [arXiv:1205.6569] [INSPIRE].

[26] L. Basso, A. Lipniacka, F. Mahmoudi, S. Moretti, P. Osland et al., *The CP-violating type-II 2HDM and Charged Higgs boson benchmarks*, PoS(Corfu2012)029 [arXiv:1305.3219] [INSPIRE].

[27] L. Basso, A. Lipniacka, F. Mahmoudi, S. Moretti, P. Osland et al., *Charged Higgs boson benchmarks in the CP-violating type-II 2HDM*, PoS(CHARGED 2012)019 [arXiv:1301.4268] [INSPIRE].

[28] A.G. Akeroyd and S. Moretti, *Enhancement of $H \to \gamma\gamma$ from doubly charged scalars in the Higgs Triplet Model*, *Phys. Rev.* **D 86** (2012) 035015 [arXiv:1206.0535] [INSPIRE].

[29] A. Celis, V. Ilisie and A. Pich, *LHC constraints on two-Higgs doublet models*, *JHEP* **07** (2013) 053 [arXiv:1302.4022] [INSPIRE].

[30] M. Krawczyk, D. Sokołowska and B. Świeżewska, *2HDM with Z_2 symmetry in light of new LHC data*, *J. Phys. Conf. Ser.* **447** (2013) 012050 [arXiv:1303.7102] [INSPIRE].

[31] J. Shu and Y. Zhang, *Impact of a CP-violating Higgs Sector: From LHC to Baryogenesis*, *Phys. Rev. Lett.* **111** (2013) 091801 [arXiv:1304.0773] [INSPIRE].

[32] C. Han, N. Liu, L. Wu, J.M. Yang and Y. Zhang, *Two-Higgs-doublet model with a color-triplet scalar: a joint explanation for top quark forward-backward asymmetry and Higgs decay to diphoton*, *Eur. Phys. J.* **C 73** (2013) 2664 [arXiv:1212.6728] [INSPIRE].

[33] J.-J. Cao, Z.-X. Heng, J.M. Yang, Y.-M. Zhang and J.-Y. Zhu, *A SM-like Higgs near 125 GeV in low energy SUSY: a comparative study for MSSM and NMSSM*, *JHEP* **03** (2012) 086 [arXiv:1202.5821] [INSPIRE].

[34] J. Cao, L. Wu, P. Wu and J.M. Yang, *The Z+photon and diphoton decays of the Higgs boson as a joint probe of low energy SUSY models*, *JHEP* **09** (2013) 043 [arXiv:1301.4641] [INSPIRE].

[35] A. Djouadi, V. Driesen, W. Hollik and A. Kraft, *The Higgs photon - Z boson coupling revisited*, *Eur. Phys. J.* **C 1** (1998) 163 [hep-ph/9701342] [INSPIRE].

[36] M. Carena, I. Low and C.E.M. Wagner, *Implications of a Modified Higgs to Diphoton Decay Width*, *JHEP* **08** (2012) 060 [arXiv:1206.1082] [INSPIRE].

[37] C.-S. Chen, C.-Q. Geng, D. Huang and L.-H. Tsai, *New Scalar Contributions to $h \to Z\gamma$*, *Phys. Rev.* **D 87** (2013) 075019 [arXiv:1301.4694] [INSPIRE].

JHEP07(2014)057

[38] ILC collaboration, G. Aarons et al., *International Linear Collider Reference Design Report Volume 2: Physics at the ILC*, arXiv:0709.1893 [INSPIRE].

[39] L. Linssen, A. Miyamoto, M. Stanitzki and H. Weerts, *Physics and Detectors at CLIC: CLIC Conceptual Design Report*, arXiv:1202.5940 [INSPIRE].

[40] TLEP Design Study Working Group collaboration, M. Bicer et al., *First Look at the Physics Case of TLEP*, *JHEP* **01** (2014) 164 [arXiv:1308.6176] [INSPIRE].

[41] G.C. Branco, P.M. Ferreira, L. Lavoura, M.N. Rebelo, M. Sher et al., *Theory and phenomenology of two-Higgs-doublet models*, *Phys. Rept.* **516** (2012) 1 [arXiv:1106.0034] [INSPIRE].

[42] S.L. Glashow and S. Weinberg, *Natural Conservation Laws for Neutral Currents*, *Phys. Rev.* **D 15** (1977) 1958 [INSPIRE].

[43] H. Fritzsch, *Calculating the Cabibbo Angle*, *Phys. Lett.* **B 70** (1977) 436 [INSPIRE].

[44] H. Fritzsch and Z.-z. Xing, *Four zero texture of Hermitian quark mass matrices and current experimental tests*, *Phys. Lett.* **B 555** (2003) 63 [hep-ph/0212195] [INSPIRE].

[45] T.P. Cheng and M. Sher, *Mass Matrix Ansatz and Flavor Nonconservation in Models with Multiple Higgs Doublets*, *Phys. Rev.* **D 35** (1987) 3484 [INSPIRE].

[46] D. Atwood, L. Reina and A. Soni, *Phenomenology of two Higgs doublet models with flavor changing neutral currents*, *Phys. Rev.* **D 55** (1997) 3156 [hep-ph/9609279] [INSPIRE].

[47] J.L. Diaz-Cruz, R. Noriega-Papaqui and A. Rosado, *Measuring the fermionic couplings of the Higgs boson at future colliders as a probe of a non-minimal flavor structure*, *Phys. Rev.* **D 71** (2005) 015014 [hep-ph/0410391] [INSPIRE].

[48] J.L. Diaz-Cruz, J. Hernandez-Sanchez, S. Moretti, R. Noriega-Papaqui and A. Rosado, *Yukawa Textures and Charged Higgs Boson Phenomenology in the 2HDM-III*, *Phys. Rev.* **D 79** (2009) 095025 [arXiv:0902.4490] [INSPIRE].

[49] J. Hernandez-Sanchez, L. Lopez-Lozano, R. Noriega-Papaqui and A. Rosado, *Couplings of quarks in the Partially Aligned 2HDM with a four-zero texture Yukawa matrix*, *Phys. Rev.* **D 85** (2012) 071301 [arXiv:1106.5035] [INSPIRE].

[50] J.F. Gunion and H.E. Haber, *The CP conserving two Higgs doublet model: The Approach to the decoupling limit*, *Phys. Rev.* **D 67** (2003) 075019 [hep-ph/0207010] [INSPIRE].

[51] J. Hernandez-Sanchez, C.G. Honorato, M.A. Perez and J.J. Toscano, *The $\gamma\gamma \to \phi_i\phi_j$ processes in the type-III two-Higgs-doublet model*, *Phys. Rev.* **D 85** (2012) 015020 [arXiv:1108.4074] [INSPIRE].

[52] A. Pomarol and R. Vega, *Constraints on CP-violation in the Higgs sector from the rho parameter*, *Nucl. Phys.* **B 413** (1994) 3 [hep-ph/9305272] [INSPIRE].

[53] J.-M. Gerard and M. Herquet, *A Twisted custodial symmetry in the two-Higgs-doublet model*, *Phys. Rev. Lett.* **98** (2007) 251802 [hep-ph/0703051] [INSPIRE].

[54] S. de Visscher, J.-M. Gerard, M. Herquet, V. Lemaitre and F. Maltoni, *Unconventional phenomenology of a minimal two-Higgs-doublet model*, *JHEP* **08** (2009) 042 [arXiv:0904.0705] [INSPIRE].

[55] S. Kanemura, Y. Okada, H. Taniguchi and K. Tsumura, *Indirect bounds on heavy scalar masses of the two-Higgs-doublet model in light of recent Higgs boson searches*, *Phys. Lett.* **B 704** (2011) 303 [arXiv:1108.3297] [INSPIRE].

JHEP07(2014)057

[56] W. Grimus, L. Lavoura, O.M. Ogreid and P. Osland, *A Precision constraint on multi-Higgs-doublet models*, *J. Phys.* **G 35** (2008) 075001 [arXiv:0711.4022] [INSPIRE].

[57] W. Grimus, L. Lavoura, O.M. Ogreid and P. Osland, *The Oblique parameters in multi-Higgs-doublet models*, *Nucl. Phys.* **B 801** (2008) 81 [arXiv:0802.4353] [INSPIRE].

[58] I.F. Ginzburg and I.P. Ivanov, *Tree-level unitarity constraints in the most general 2HDM*, *Phys. Rev.* **D 72** (2005) 115010 [hep-ph/0508020] [INSPIRE].

[59] J. Hernandez-Sanchez, S. Moretti, R. Noriega-Papaqui and A. Rosado, *Off-diagonal terms in Yukawa textures of the Type-III 2-Higgs doublet model and light charged Higgs boson phenomenology*, *JHEP* **07** (2013) 044 [arXiv:1212.6818] [INSPIRE].

[60] J. Hernandez-Sanchez, S. Moretti, R. Noriega-Papaqui and A. Rosado, *Update of the 2HDM-III with a four-zero texture in the Yukawa matrices and phenomenology of the charged Higgs Boson*, PoS(CHARGED 2012)029 [arXiv:1302.0083] [INSPIRE].

[61] O. Félix-Beltrán, F. González-Canales, J. Hernández-Sánchez, S. Moretti, R. Noriega-Papaqui et al., *Analysis of the quark sector in the 2HDM-III with a four-zero Yukawa texture using the most recent data on the CKM matrix*, arXiv:1311.5210 [INSPIRE].

[62] Y. Grossman, *Phenomenology of models with more than two Higgs doublets*, *Nucl. Phys.* **B 426** (1994) 355 [hep-ph/9401311] [INSPIRE].

[63] A.G. Akeroyd, S. Moretti and J. Hernandez-Sanchez, *Light charged Higgs bosons decaying to charm and bottom quarks in models with two or more Higgs doublets*, *Phys. Rev.* **D 85** (2012) 115002 [arXiv:1203.5769] [INSPIRE].

[64] M. Aoki, S. Kanemura, K. Tsumura and K. Yagyu, *Models of Yukawa interaction in the two Higgs doublet model and their collider phenomenology*, *Phys. Rev.* **D 80** (2009) 015017 [arXiv:0902.4665] [INSPIRE].

[65] A. Djouadi, *The Anatomy of electro-weak symmetry breaking. I: The Higgs boson in the standard model*, *Phys. Rept.* **457** (2008) 1 [hep-ph/0503172] [INSPIRE].

[66] A. Crivellin, A. Kokulu and C. Greub, *Flavor-phenomenology of two-Higgs-doublet models with generic Yukawa structure*, *Phys. Rev.* **D 87** (2013) 094031 [arXiv:1303.5877] [INSPIRE].

[67] M. Carena, T. Han, G.-Y. Huang and C.E.M. Wagner, *Higgs Signal for $h \to aa$ at Hadron Colliders*, *JHEP* **04** (2008) 092 [arXiv:0712.2466] [INSPIRE].

[68] J.F. Gunion, H.E. Haber, G.L. Kane and S. Dawson, *The Higgs Hunter's Guide*, Addison-Wesley, Reading, MA (1990).

[69] W.-Y. Keung and W.J. Marciano, *Higgs scalar decays: $H \to W^{\pm} + X$*, *Phys. Rev.* **D 30** (1984) 248 [INSPIRE].

[70] E. Barradas, J.L. Diaz-Cruz, A. Gutierrez and A. Rosado, *Three body decays of Higgs bosons in the MSSM*, *Phys. Rev.* **D 53** (1996) 1678 [INSPIRE].

[71] J.L. Diaz-Cruz and M.A. Perez, *Decays of Heavy Charged Higgs Bosons*, *Phys. Rev.* **D 33** (1986) 273 [INSPIRE].

[72] M. Gomez-Bock and R. Noriega-Papaqui, *Flavor violating decays of the Higgs bosons in the THDM-III*, *J. Phys.* **G 32** (2006) 761 [hep-ph/0509353] [INSPIRE].

JHEP07(2014)057